In-plane elastic constants of a new curved cell walls honeycomb concept

Amine Harkati, Djamel Boutagouga, El-Hadi Harkati, Abderrezak Bezazi, Fabrizio Scarpa, Morvan Ouisse

In-plane elastic constants of a new curved cell walls honeycomb concept

A. Harkati[1], D. Boutagouga[1], E. Harkati[1], A. Bezazi[2], F. Scarpa[3], M. Ouisse[4]
[1]Université de Larbi Tébessi, Laboratoire des mines, route de Constantine, Tébessa 12002, Algérie.
[2] Laboratoire Mécanique appliquée des nouveaux matériaux (LMANM), B.P 401 Université 8 Mai 1945 Guelma, Algérie.
[3]Bristol Composites Institute (ACCIS) and Dynamics and Control Research Group (DCRG), University of Bristol, BS8 1TR Bristol, UK.
[4]Univ. Bourgogne Franche Comté, FEMTO-ST Institute, CNRS/UFC/ENSMM/UTBM, Department of Applied Mechanics, 24 rue de l'épitaphe, 25000, Besançon, France

Abstract

This paper is focused on the identification of the in-plane elastic constants of a new design of auxetic (negative Poisson's ratio) honeycomb configuration with curved cell walls by using analytical and numerical homogenization techniques. The sensitivity of the elastic constants is determined against the various cell geometry parameters. Good agreement between the analytical and numerical simulations is observed. We show that the specific curved wall honeycomb configuration proposed in this paper possesses a high in-plane shear compliance, tailored anisotropy and the possibility of inducing a negative Poisson's ratio behaviour in baseline honeycomb configurations that would have otherwise positive in-plane Poisson's ratios.

Keyword: honeycomb, homogenization, curvature walls, elasticity moduli, auxetic, refined model

NOTATIONS

A : Basic wall transverse section.
E_1, E_2: Young's modulus in directions 1 and 2.
G_{12} : shear modulus
v_s : Poisson's ratio of basic material.
E_s : Young's modulus of basic material.
l : Cell wall length.
v_{12}, v_{21}: In-plane Poisson's ratios.
ε_1, ε_2: Plane strains in directions 1 and 2.
θ : Cell internal angle.
r : curved of the basic wall.
a : cell wall base
t : Cell wall thickness.
U : Elastic strain energy.
u_1, u_2 : Displacement in directions *1* and *2* respectively.
b : Height of the cell.
α: curvature ratio, $\left(\alpha = r/l\right)$.
β : Basic wall aspect ratio, $\left(\beta = a/l\right)$.
γ : Basic wall thickness ratio, $\left(\gamma = t/l\right)$

1. Introduction

Low density cellular materials are mainly used as a lightweight core rigid and high strength sandwich structures. The physical properties of these materials depend on their constituent phase, geometry and spatial arrangement of the solid [1]. This type of porous structure has several applications in the civil and military fields that require both rigidity and lightweight characteristics. An example of cellular material used as lightweight core is the corrugated paper honeycomb [2], which can be used as a base material in lightweight and low-cost sandwich elements. The moduli of elasticity, the shear and compression strengths have been determined in that work both experimentally and analytically, showing that the mechanics of the impregnated material are more consistent than the ones of non-impregnated cellular solids. It is therefore interesting to evaluate their mechanical properties and predict their behaviour under specific loading and environments. Several research studies on such systems have been carried out in recent years, particularly about tailored two-dimensional honeycombs. Asymptotic homogenization constitutes a means to replace full-scale simulations for predicting the equivalent mechanical properties of the lattices [3-9].

The term auxetics indicates structures and materials with negative Poisson's ratio characteristics. Evans and al. [10] have been the first to use this term (from the word ''auxetos", i.e. 'may be subjected to increase'). In most cases, the Poisson's ratio of cellular structures is positive, i.e. the material undergoes a contraction along the direction perpendicular to one of the load applications. However, a negative value of the Poisson's ratio means that the material would laterally expand when stretched, leading to an increase of its volume [11-13]. A class of foams that exhibited negative Poisson's ratios has been manufactured and presented for the first time by Lakes [14] back in 1987. The first model of re-entrant structures with a negative Poisson's ratio was introduced back in 1985 by Almgren [15]. The structure was first made in 2 D before being extended to 3D. That pattern, which may be applied to different geometric structures such as rods, hinges, and springs led to the development of structures that show macroscopic isotropic elastic properties though anisotropic in their microscopic details. Lira and al. [16] described the out-of-plane shear properties of the multi re-

entrant honeycomb configurations. The transverse shear strength properties of zero-Poisson's ratio honeycombs have been described in [17]. The transverse shear modulus of honeycombs with negative Poisson's ratio coefficients in the plane have been determined using numerical simulations by [18].

The mechanics of re-entrant and centre-symmetric honeycomb configurations has been described using various analytical models, which have been essentially based on the hypothesis that the behaviour of individual beams or ribs of the cell can be described by elastic engineering beams, specific sets of boundary conditions and different cell walls mechanisms (stretching/hinging/bending [19]). When loaded on a plane, the honeycomb-shaped cells may be subjected to bending or stretching of their walls, as well as the rotations of the connecting junctions (nodes). Several researchers have developed mathematical models based on these mechanisms. Gibson and Ashby [1] and Gibson and al. [19] developed a 2-D model assuming a beam-like bending of the cell walls. Nkansah and Hutchinson [18] however showed that models solely based on bending tend to misrepresent the in-plane elastic constants of honeycombs for small (positive and/or negative) cell angles. In order to improve the bending-based models, Gibson et al [19] and Masters and Evans [20] incorporated the phenomena of stretching and rotation of the cell walls. Earlier studies focused on the regular hexagonal honeycomb used as the base material for sandwich panels. In-plane properties are widely studied to improve knowledge of the mechanical behaviour of cellular materials. Advances in shell theories and increasing computational power have improved the models already described by elementary theories. Numerous numerical homogenization techniques have been proposed for modelling network materials (see Arabnejad and Pasini [21]). A comprehensive review about homogenization methods applied to honeycomb structures was presented in [22] but did not report the effect of the curvature of the wall at the junctions. Within the last two decades, the availability of faster and more sophisticated manufacturing techniques has pushed the development of new cell geometries to meet the needs of technological users.

Works from Harkati et al. [4] and Balawi and Abot [23] have proposed a general analytical model to predict the elastic moduli applied to a hexagonal cell with curved walls. The model has allowed the parametrization of the elastic modulus and relative density as a function of the radius of curvature and other cell geometry characteristics. The model takes into account the effects of bending, shear and

axial deformations of the cell ribs along the two principal directions of the plane, and especially confirmed that the curvature of the walls does not have the same effect along each direction. Malek and Gibson [24] have studied the elastic behaviour of periodic hexagonal honeycombs over a wide range of relative densities and cell geometries by taking into account nodes at the intersection of vertical and inclined elements.

This article proposes a refined analytical model capable to evaluate the effect of the curvature of the cell wall and the internal cell angle on the in-plane mechanical behaviour of honeycomb cells defined by five homogenized elastic modules, taking into account different types of deformation mechanisms in the plane. Fig. 1(a) presents the configuration investigated in this work, in which the sharp edge corners are replaced by rounding of radius *r*. Fig. 1(b) shows a previous multi-re-entrant configuration evaluated by some of the Authors [2-5], while Fig. 1(c) is related to the baseline centre-symmetric honeycomb structure [1].

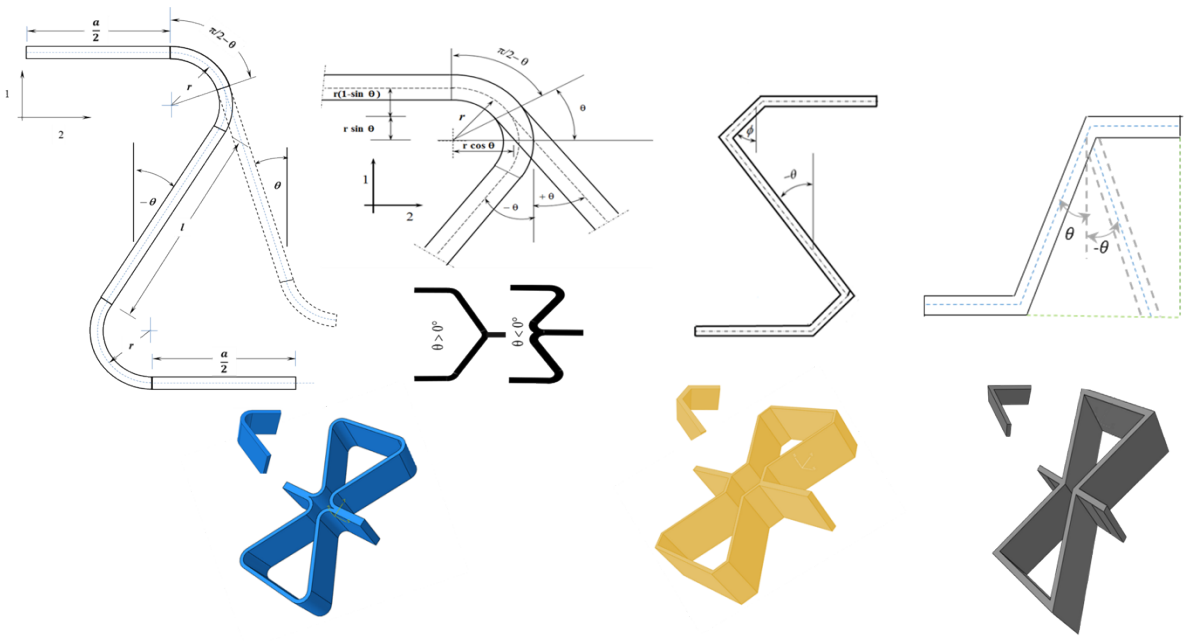

(a) (b) (c)

Figure 1: Honeycomb architectures

a): Present work b): Previous Authors' work [5] c): regular hexagonal

This work is based on the methodologies and results presented in Refs. [3-6]. The main novelties introduced here consist in the determination of the in-plane shear modulus (G_{12}) by analytical means,

and the development of a refined model that imposes geometric constraints to avoid the contact of the curved walls during deformation. The models are validated using three-dimensional Finite Element models including asymptotic homogenization conditions. The variation of the Poisson's ratio versus the radius of curvature ratio (α=r / l) for three honeycomb configurations (straight walls, multi-reentrant and the one described here) and the evolution of the anisotropy versus the curvature ratio of the walls has been identified and discussed. The curved wall honeycomb cell configuration described by these models shows a very high degree of compliance, especially in terms of shear deformation. Quite importantly, the tailoring of the radius of curvature shows that it is possible to control the degree of anisotropy and the development of auxeticity in baseline honeycomb configurations (i.e., with straight walls) that would normally exhibit a positive Poisson's ratio behavior.

2. Theoretical analysis

2.1 Refined analytical model

The analytical model developed here is based on Castigliano's theorem. The honeycomb cell walls are considered as beam elements and simultaneously subjected to three types of loading (bending, membrane and shear - Fig. 1). In order to avoid contacts and intersections of the cell walls during the deformation the condition below is applied:

$$a > 2l\sin\theta + 2r\left(1-2\cos\theta\right) \tag{1}$$

According to elastic beam theory, the elastic strain energy U is expressed as [4]:

$$U = U_M + U_N + U_T = \int_0^l \left(\frac{N^2}{2EA} + \frac{M^2}{2EI} + \frac{T^2}{2GA^*} \right) dx \tag{2}$$

Where N is the axial internal force, T is the shear internal force and M is the internal bending moment. In (2) E is the material's Young's Modulus, G is the shear modulus, A is the cross-section area, A^* is the shear reduced area, I is the area moment of inertia and l is the beam length.

The displacement of a beam under the influence of a force P may be expressed as $u = \frac{\partial U}{\partial P}$.

The mathematical formulation of the expressions providing the modules E_1, E_2, v_{12} and v_{21} are detailed in previous Authors' paper [3]. The equations are recalled here with E_s the elastic modulus of the base material.

$$\frac{E_1}{E_s} = \frac{\cos\theta+2\alpha(1-\sin\theta)}{\beta+\sin\theta+2\alpha\cos\theta}\frac{1}{\bar{u}_1} \tag{3}$$

With: $\beta = a/l$

$$\bar{u}_1 = \frac{1}{\gamma^3}\left[\begin{pmatrix} 6\left(\pi-2\theta-8\cos\theta+6\cos\theta\sin\theta+(2\pi-4\theta)\cos^2\theta\right)\alpha^3 \\ +12\left(2-2\sin\theta-2\cos^2\theta+(\pi-2\theta)\cos\theta\sin\theta\right)\alpha^2 \\ +3\left(\pi-2\theta-(\pi-2\theta)\cos^2\theta\right)\alpha+\sin^2\theta \end{pmatrix} + \begin{pmatrix} \frac{1}{2}\gamma^2\left(1-2\alpha\theta+\cos 2\theta-\alpha\sin 2\theta+\pi\alpha\right) \\ +\frac{6(1+\nu)}{5}\gamma^2\left(1-2\alpha\theta-\cos 2\theta+\alpha\sin 2\theta+\pi\alpha\right) \end{pmatrix}\right] \tag{4}$$

For a regular cell $\alpha=0$ (Gibson and Ashby's advanced equation for honeycomb [1])

$$\frac{E_1}{E_s} = \gamma^3\,\frac{\cos\theta}{(\alpha+\sin\theta)\sin^2\theta}\left(\frac{1}{1+\gamma^2(\cot^2\theta+\frac{12}{5}(\nu+1))}\right) \tag{5}$$

The apparent modulus in direction 2 writes

$$\frac{E_2}{E_s} = \frac{\beta+\sin\theta+2\alpha\cos\theta}{\cos\theta+2\alpha(1-\sin\theta)}\frac{1}{\bar{u}_2} \tag{6}$$

with

$$\bar{u}_2 = \frac{1}{\gamma^3}\left[\begin{bmatrix} (12\pi-24\theta-18\sin 2\theta-6\pi\cos 2\theta+12\theta\cos 2\theta)\alpha^3 \\ +(12+12\cos 2\theta-6\pi\sin 2\theta+12\theta\sin 2\theta)\alpha^2 \\ +(\frac{3}{2}\pi-3\theta+\frac{3}{2}\pi\cos 2\theta-3\theta\cos 2\theta)\alpha \\ \cos^2\theta \end{bmatrix} + \begin{Bmatrix} \frac{1}{2}\gamma^2\left(1-2\alpha\theta-\cos 2\theta+\alpha\sin 2\theta+\pi\alpha+4\beta\right) \\ +\frac{6(1+\nu)}{5}\gamma^2\left(2\cos^2\theta-2\alpha\theta-\alpha\sin 2\theta+\pi\alpha\right) \end{Bmatrix}\right] \tag{7}$$

Also, in this case, by imposing $\alpha = 0$ we obtain the result related to a regular hexagonal cell:

$$\frac{E_2}{E_s} = \gamma^3\,\frac{\alpha+\sin\theta}{\cos^3\theta}\left(\frac{1}{1+\gamma^2\left(\tan^2\theta+\frac{12}{5}(\nu+1)\right)}\right) \tag{8}$$

The Poisson's ratio of the honeycomb is provided by the following expression :

$$v_{12} = -\frac{\cos\theta+2\alpha(1-\sin\theta)}{\sin\theta+(\beta+2\alpha\cos\theta)}\left(\frac{\begin{Bmatrix} 6\alpha^3(3\cos 2\theta+4\sin\theta-\pi\sin 2\theta+2\theta\sin 2\theta-1) \\ +6\alpha^2(2\sin 2\theta-2\cos\theta+(\pi-2\theta)\cos 2\theta) \\ +\frac{3}{2}\alpha(\pi-2\theta)(\sin 2\theta)+\frac{1}{2}\sin 2\theta \end{Bmatrix} + \begin{Bmatrix} -\frac{1}{2}\gamma^2(\alpha+\alpha\cos 2\theta+\sin 2\theta) \\ +\frac{6(1+\nu)}{5}\gamma^2(\alpha+\alpha\cos 2\theta+\sin 2\theta) \end{Bmatrix}}{\begin{Bmatrix} 6\alpha^3\left((\pi-2\theta)(1+2\cos^2\theta)-8\cos\theta+6\cos\theta\sin\theta\right) \\ +12\alpha^2\left(2\sin^2\theta-2\sin\theta+(\pi-2\theta)\cos\theta\sin\theta\right) \\ +3\alpha\left((\pi-2\theta)\sin^2\theta\right)+\sin^2\theta \end{Bmatrix} + \begin{Bmatrix} \frac{1}{2}\gamma^2(1-2\alpha\theta+\cos 2\theta-\alpha\sin 2\theta+\pi\alpha) \\ +\frac{6(1+\nu)}{5}\gamma^2(1-2\alpha\theta-\cos 2\theta+\alpha\sin 2\theta+\pi\alpha) \end{Bmatrix}}\right) \tag{9}$$

Finally, the Poisson's ratio v_{21} can be calculated as:

$$\nu_{21} = \frac{E_1}{E_2}\nu_{12} \tag{10}$$

2.2 Shear modulus

Because of symmetry, there is no relative motion between points A, B and C when the honeycomb is sheared (see Fig. 2).

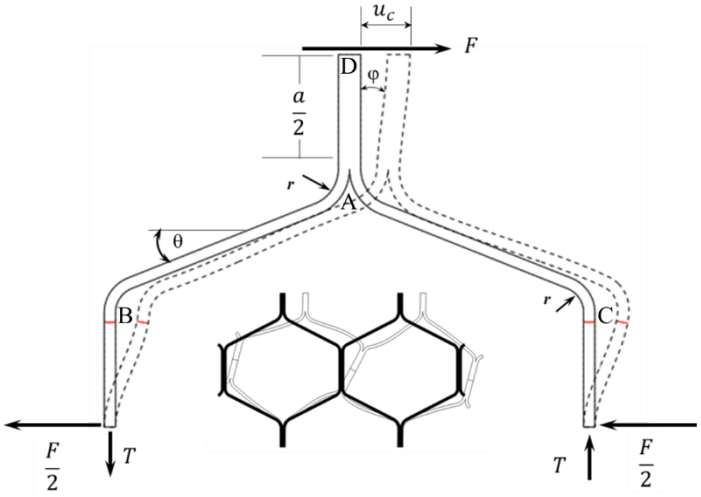

Figure 2: Deformation induced by cell wall bending and rotation - Force distribution to evaluate G_{12}.

The shear deflection u_c is due to the horizontal displacement of point A, and bending of beam AD and its rotation through the angle φ at around A point [1].

The rotation angle φ can be then expressed by the following formula:

$$\varphi = \frac{1}{24EI}\frac{Fal^3}{\left(l+2r-2r\sin\theta\right)^2}\langle\bar{u}\rangle \tag{11}$$

With: $$\langle\bar{u}\rangle = \begin{bmatrix} 1+(6\pi-12\theta-12\cos\theta-24\sin\theta+6\pi\sin\theta-12\cos^2\theta-12\theta\sin\theta-12\cos\theta\sin\theta+24)\frac{r^3}{l^3} \\ +(18+6\cos\theta-18\sin\theta-3\pi\sin\theta+6\theta\sin\theta)\frac{r^2}{l^2}+(3\pi-6\theta)\frac{r}{l} \end{bmatrix} \tag{12}$$

The shear displacement u_c (shearing deflection) can be presented as:

$$u_c = \frac{Fa^2}{48EI}\left(\frac{l^3}{\left(l+2r-2r\sin\theta\right)^2}\langle\bar{u}\rangle+2a\right) \tag{13}$$

The shear strain γ_{12} is given by:

$$\gamma_{12} = \frac{2u_c}{\left(a + l\sin\theta + 2r\cos\theta\right)} = \frac{Fa^2}{24EI\left(a + l\sin\theta + 2r\cos\theta\right)}\left(\frac{l^3}{\left(l + 2r - 2r\sin\theta\right)^2}\langle\hat{u}\rangle + 2a\right) \tag{14}$$

One can then calculate the shear stress τ.

$$\tau = \frac{F}{2b(l\cos\theta + 2r(1-\sin\theta))} \tag{15}$$

After mathematical manipulations and using non-dimensional parameters, one can obtain the expression of G_{12}:

$$G_{12} = \frac{\tau}{\gamma_{12}} \tag{16}$$

$$\frac{G_{12}}{E_s} = \left(\frac{t}{l}\right)^3 \frac{\left(\beta + \sin\theta + 2\alpha\cos\theta\right)}{\left(\cos\theta + 2\alpha\left(1-\sin\theta\right)\right)\beta^2} \frac{1}{\left(2\beta + \frac{1}{\left(1 + 2\alpha - 2\alpha\sin\theta\right)^2}\langle\hat{u}\rangle\right)} \tag{17}$$

For $\alpha = 0$ one can obtain the value the in-plane shear modulus of a regular hexagonal honeycomb [1]:

$$\frac{G_{12}}{E_s} = \left(\frac{t}{l}\right)^3 \frac{\left(\beta + \sin\theta\right)}{\beta^2\left(2\beta + 1\right)\left(\cos\theta\right)} \tag{18}$$

2.3. Finite element modelling

In order to validate the results found by the analytical approach, numerical models based on finite elements method were developed using the ABAQUS commercial code [25]. The models developed here are based on studies and simulations performed by several authors [1-6, 16, 26, 27]. The first model considers full-scale honeycomb assemblies of 53 mesh cells with quadratic beam elements (8304 elements - 3 nodes quadra

tic beams in a plane), while the second one involves the use of 68 mesh cells with 69904 shells elements with 4 nodes and 6 degrees of freedom per node (S4R). The different meshes correspond to different numerical convergence reached by using beam and shell elements when simulating the five elastic constants. The simulation of a tensile stress along the 1-direction provides the elastic modulus E_1 and the Poisson's ratio ν_{12} (Figure 3.a). The application of a tensile stress along the 2-direction allows to predict the elastic modulus E_2 and the Poisson's ratio ν_{21} (Figure 3.b). The shear stress is

simulated in the xy plane to determine the shear modulus G_{12} according to the boundary conditions in Figure 3.c.

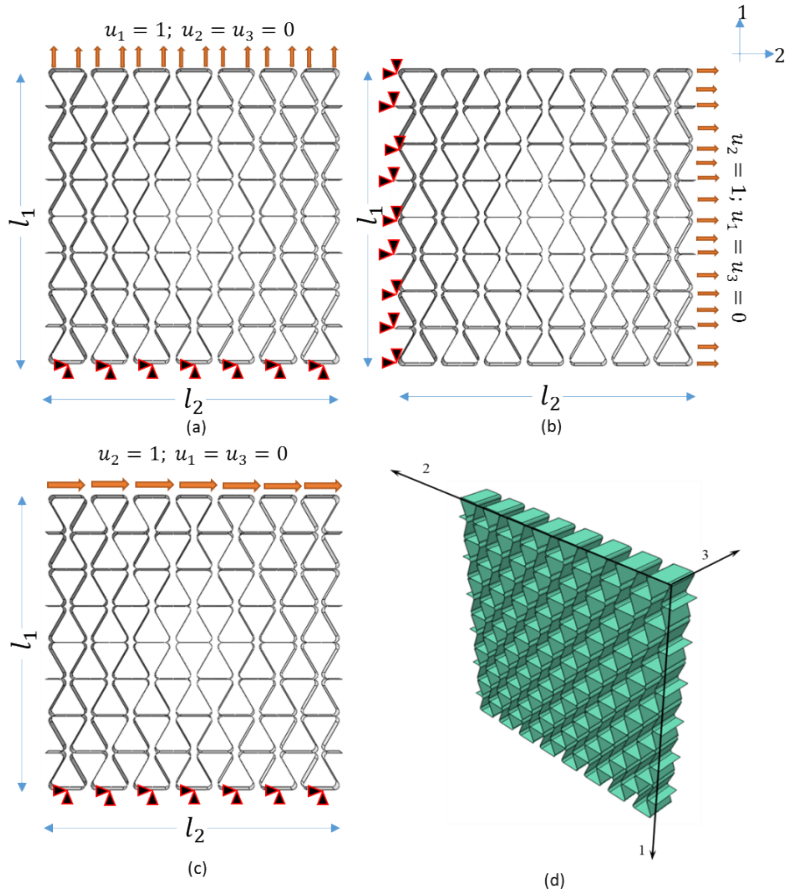

Figure 3: Numerical model description. (a) and (b) Boundary conditions taken in the simulation of the tensile along direction 1 and 2 respectively. (c) Boundary condition taken in order to determine G_{12} . (d) REV

3. Results and discussion

3.1 Effect of the curvature on the uniaxial moduli E_1 and E_2

The variation of the relative elastic modulus (E_1/E_S) as a function of the internal angle of the cell θ for different values of the ratio of the wall curvature radius $\alpha = r/l =$ (0, 0.1, 0.2 to 0.6) is shown in figure 4. In this case the non-dimensional geometrical parameters $\beta=a/l$ and $\gamma=t/l$ are fixed and equal to 1 and 0.05 respectively. The nondimensional modulus E_1/E_S decreases with the increase of α and reaches a maximum value for θ between -14 and -3 degrees; this is valid for every cell wall curvature ratio considered. The increase of θ leads to the decrease of E_1/E_S until a minimum value for every

honeycomb configuration here considered, and the maximum values all correspond to values of θ close to zero.

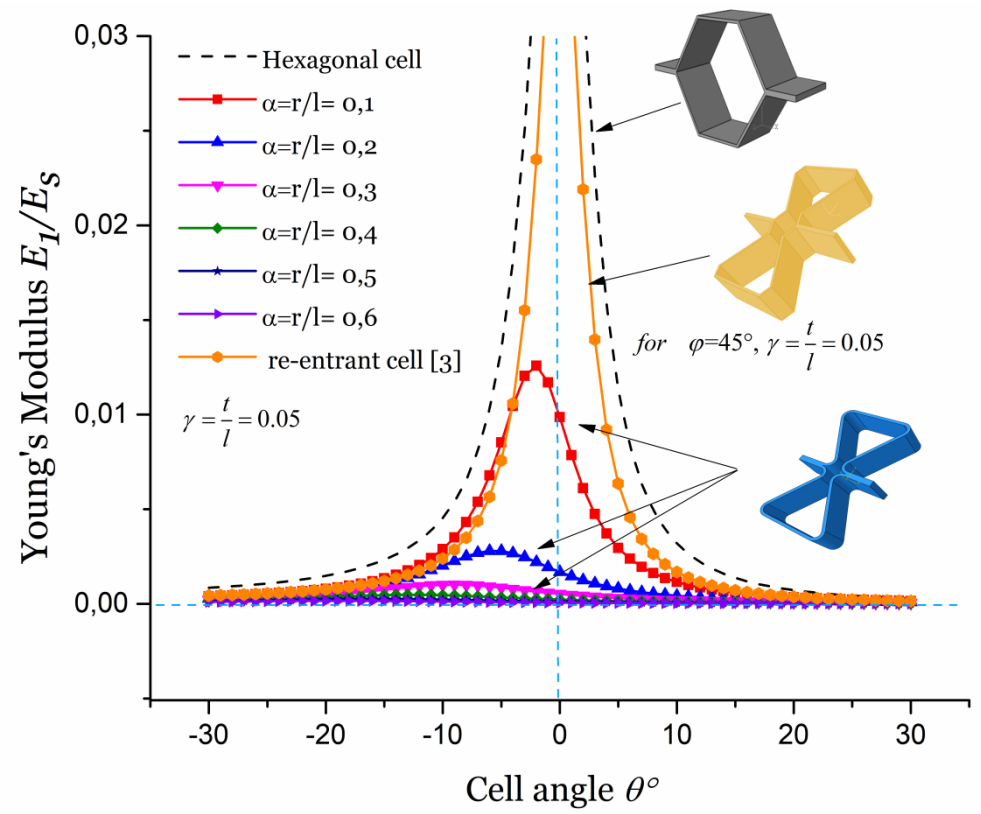

Figure 4: Normalized effective elastic modulus in 1-direction E_1 / Es versus cell angle for different normalized radius of curvature ratios (β =1 ,γ=0.05).

The maximum value of E_1/E_S for cells with curvature is typically located in the negative range of its internal angles, and it decreases with increasing angles. Increased radius of curvature ratios from r/l = 0 to r/l = 0.6 extend the range of the internal angles of cell θ, and the auxetic behaviour only occurs when θ > -5 degrees. Reducing r to zero, one can obtain the in-plane Young's modulus for the classical centre symmetric configuration.

For a zero-wall curvature ratio the value of E_1/E_S is respectively 3.33 and 3.72 times greater than for α equal to 0.1 and 0.6 for β = 1, γ = 0.05. This shows that as the radius of curvature increases the cell walls become more and more flexible. Hexagonal regular honeycomb configurations have higher Young's modulus (E_1/E_S) than topologies with or without curvature, especially within the [−5° , 5°] interval.

By fixing the non-dimensional geometrical parameters constant (β = 1 and γ = 0.05), the variation of the non-dimensional elasticity modulus of (E_2/E_s) with the wall curvature ratio is quasi-parabolic (Figure 5), particularly for internal positive cell angles. Moreover, E_2/E_s reaches its maximum for θ equal to 30 degrees in all the honeycomb cells studied here. The highest values are obtained for α equal to zero, which corresponds to a conventional hexagonal cell. The flexibility of the cells is proportional to the radius of curvature of the cell walls when the honeycomb is loaded along the 2 direction. Furthermore, the re-entrant cell without curvature (see [2]) is more rigid since it has E_2/E_s higher than the one proposed in this work (with curvature).

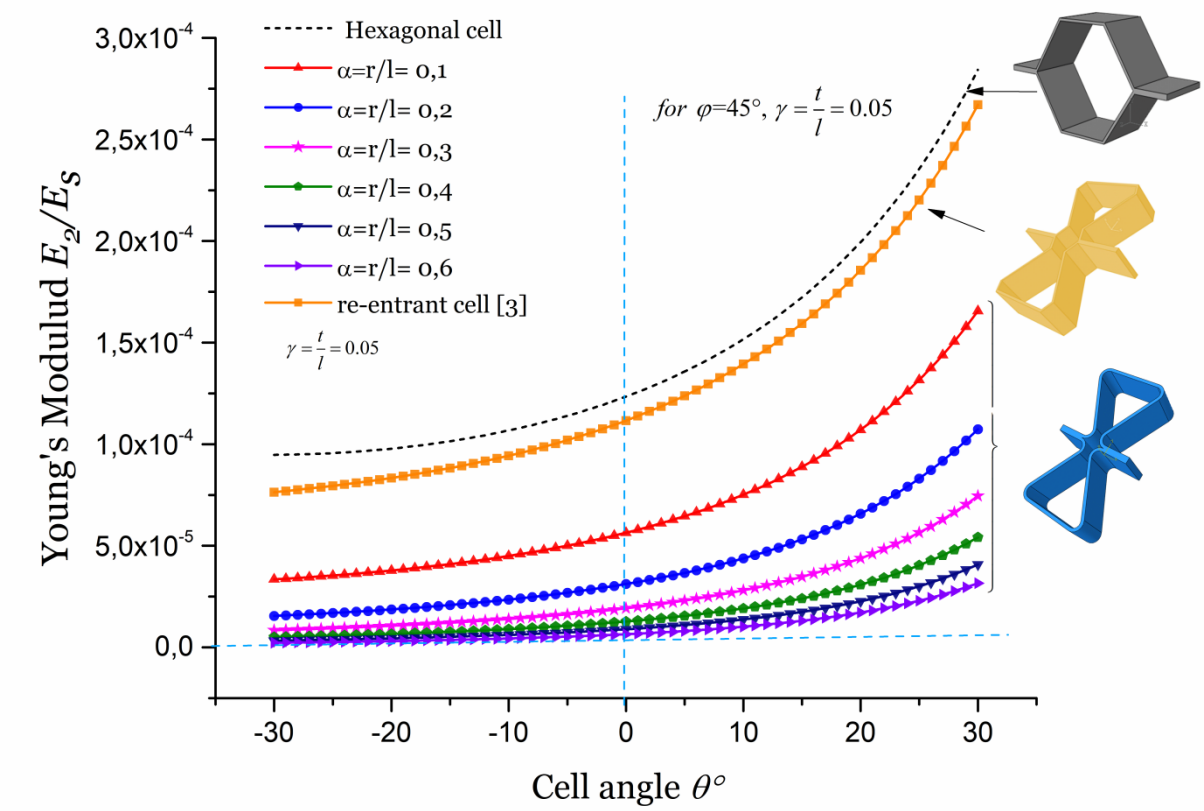

Figure 5: Normalized effective elastic modulus in 2-direction E_2/Es versus cell angle for different normalized radius of curvature (β =1 ,γ=0.05)

3.2 Effect of the curvature on the Poisson's ratios (ν_{12} and ν_{21})

The variation of the Poisson's ratios with the curvature ratio of the cell wall and the internal cell angle is shown in Figure 6. One can notice the decrease of ν_{12} when the wall curvature ratio increases. It is also important to observe that the curvature causes a widening of the conventional behaviour of the cell (i.e., positive Poisson's ratio), even for negative internal angles. The maximum value of the

Poisson's ratios (ν_{12}) corresponds to a regular hexagonal cell (α=0), and it is equal to 9.49 and -10.54 respectively for θ equal to 3 and -3 degrees. Cells without curvature [2] lead to ν_{12} values equal to 8.51 and -9.01 respectively, for θ equal to 2 and -2 degrees. The cell with the curved base walls presented in this work shows however positive and the negative values for ν_{12} equal to 7.40 and -7.84 in the cases of r/l of 0.1, and for θ equal to 2 and -7 degrees respectively.

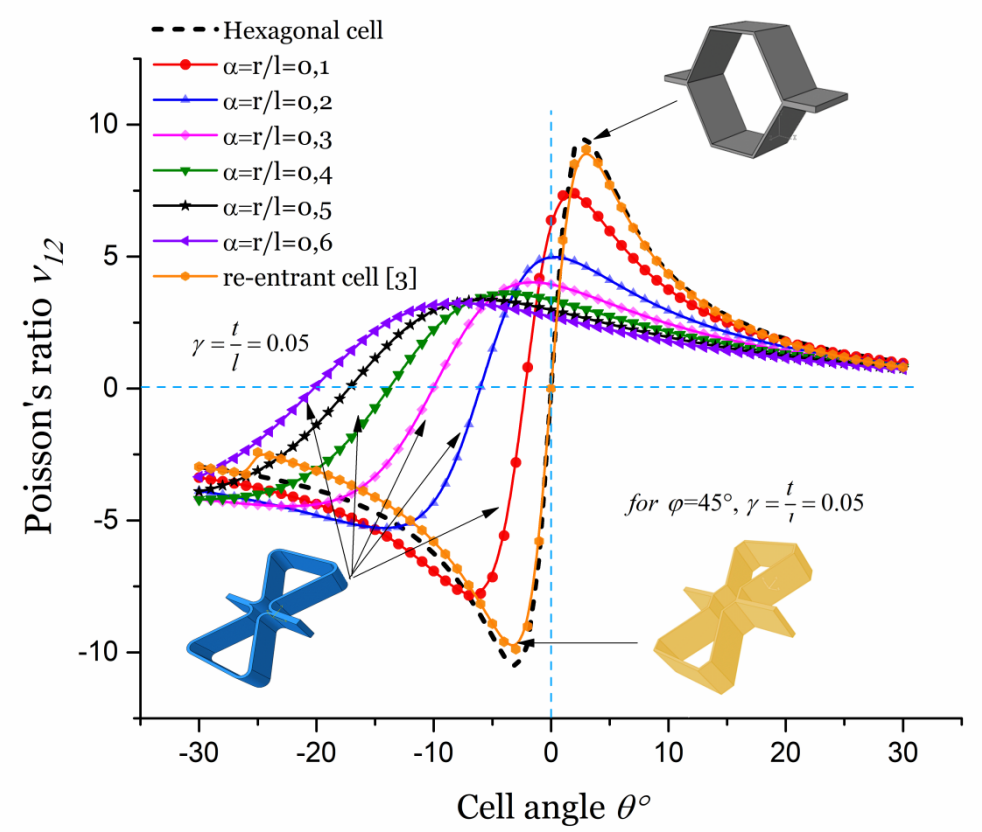

Figure 6: Poisson's ratio ν_{12} versus cell angle for different normalized radius of curvature for (β =1, γ=0.05).

Figure 7 shows the evolution of the Poisson's ratio ν_{21} versus the internal cell angle for different curvature ratios α from 0.1 to 0.6, with an increment of 0.1. The ν_{21} values decrease with increasing radius of curvature for every honeycomb configuration considered here, with and without the curved walls. Classical honeycombs can have a negative Poisson's ratio from smaller negative values of θ reach the minimum of ν_{21} (-0.33) to for θ = -30°. The maximum positive Poisson's ratio is however equal to 0.96 for θ = 30°. It is important to note that the configuration without the corner is practically similar to the classical configuration, however the honeycomb cell with curved corners shows a

negative Poisson's ratio depending on the α parameter. Indeed, for α = 0.1 the topology has a ν_{21} = -0.012 when θ equal 3 degrees until it reaches a minimum equal to -0.28 for $\theta = -30$. For α = 0.6 ν_{21} is equal to -0.0065 at $\theta = -21^{o}$, and the minimum equals to -0.069 when $\theta = -30$.

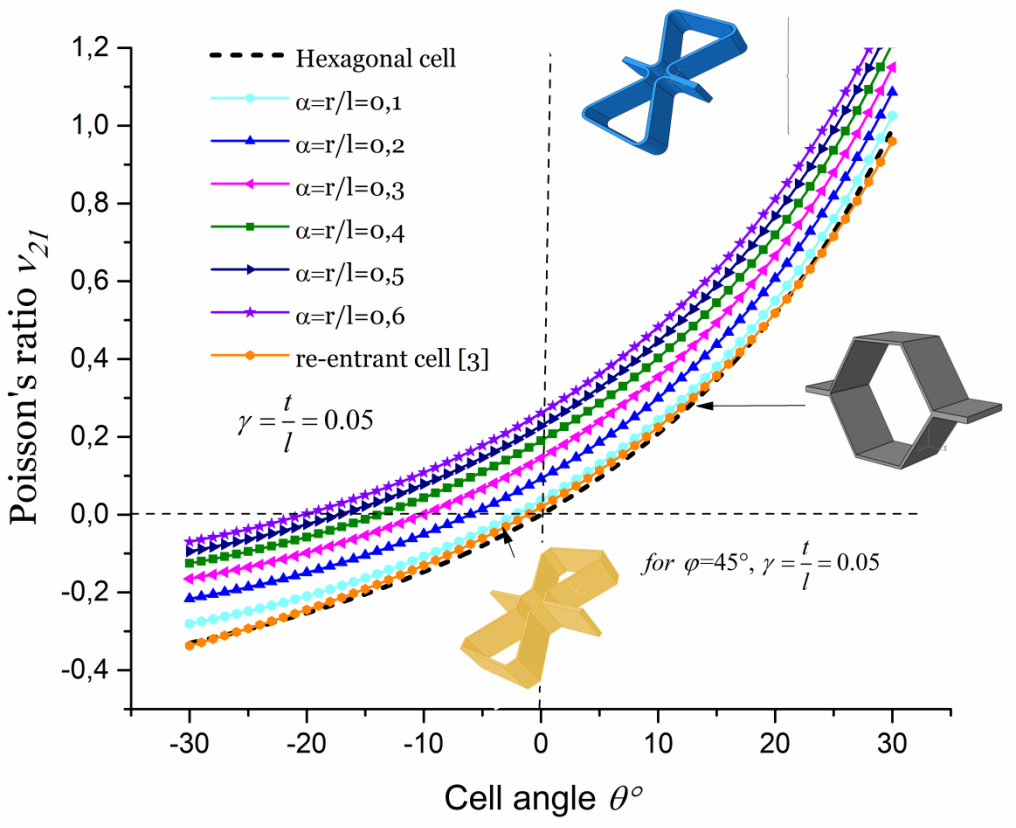

Figure 7: Poisson's ratio ν_{21} versus cell angle for different normalized radius of curvature for (β =1, γ=0.05).

The variation of the Poisson's ratio ν_{21} for the extreme internal cell angles considered here (-30 °, 0 ° and + 30 °) with the different relative curvatures of the walls varying from r/l = 0.1 to 0.6 with a step of 0.05 is presented in figure 8. The figure also considers fixed parameters of β= a/l = 1 and γ = t/l = 0.05. The value of the Poisson's ratio ν_{12} decreases with the increase of the radius of curvature α: for θ=0° and 30° and α varying from 0.1 to 0.6 the values of ν_{12} drop from to 6.5 to 2.75, and from 5.4 to -0.25 respectively. At the same time for θ equal -30° the Poisson's ratio ν_{12} decreases from -3.34 until its minimum value of -4.25 for α varying from 0.1 to 0.35. After that point the Poisson's ratio increases until it reaches its maximum of 3.35 when α is equal to 0.6.

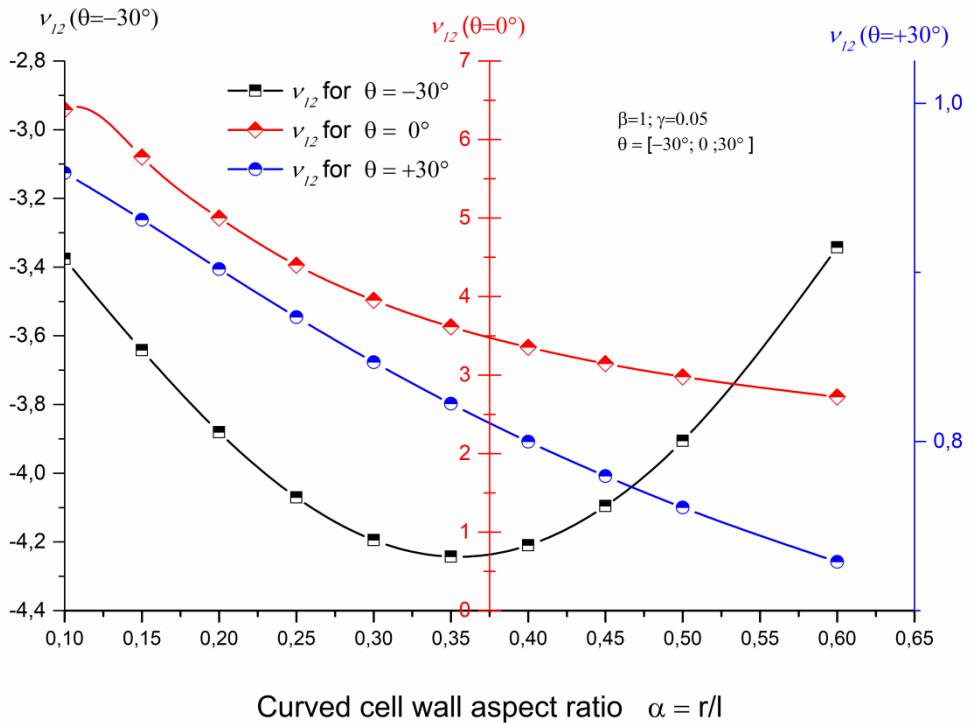

Figure 8. Poisson's ratio ν_{12} versus curvature radius ratio ($\alpha = r/l$) for the three configurations (θ equal to −30, 0 and +30 degrees).

3.3 Effect of the curvature on the shear modulus G_{12}

Figure 9 represents the variation of the shear modulus G_{12}/E_s normalized as a function of the cell angle for different radiuses of the wall curvature α (0.1 to 0.6 with step of 0.1) and fixing the value of $\beta = a/l = 1$ and $\gamma = t/l = 0.05$. The normalized shear modulus G_{12}/E_s decreases with the increase of the radius of curvature α and reaches the maximum and minimum values respectively for θ equal to 30 and -30 degrees. These results indicate that compliant honeycombs in shear can be designed by using large negative internal cell angles and large curvature values. The maximum value of the shear modulus corresponds to a regular hexagonal cell (α=0). The variation of (G_{12}) with the wall curvature ratio is quasi-parabolic (Figure 9) especially for conventional cell configurations, and the shear modulus decreases by a factor of 3 when wall curvature ratios change from 0 to 0.6. This may constitute disadvantage for structural applications for which a high shear modulus in the plane is required. However, this is a potentially useful feature for compliance-based applications, such as morphing skin with high shear deformability [28-29]. Moreover, the variation of the in-plane shear

modulus versus the constitutive geometry parameters shows that the re-entrant cell without rounding (multi-re-entrant [3]) features higher shear stiffnesses than those from the curved wall cells described in this work, but lower than those exhibited by a conventional hexagonal cell.

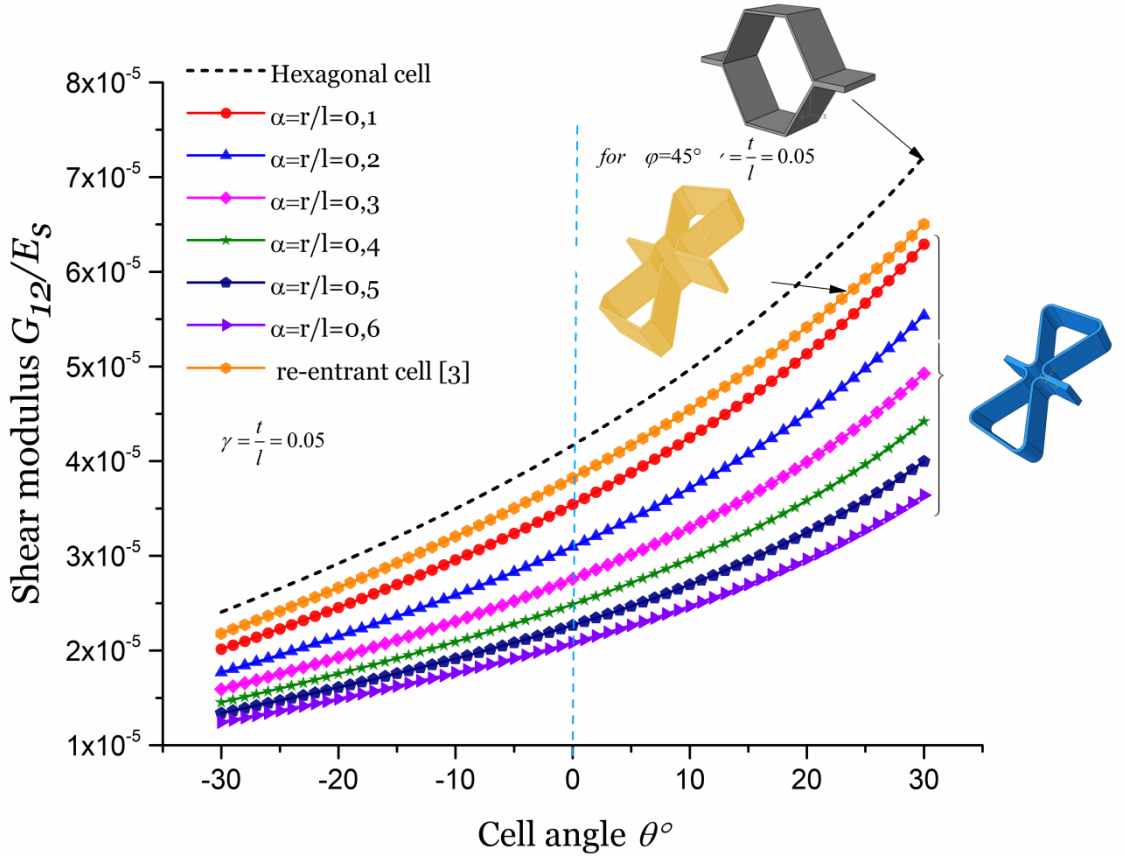

Figure 9: Normalized effective shear modulus G_{12}/Es versus cell angle for different normalized radius of curvature (β =1 ,γ=0.05).

Figure 10 shows a surface map of the normalized shear modulus G_{12}/Es as a function of the two parameters α and θ. It can also be noticed that the difference in values of the shear modulus between the two configurations (auxetic and conventional) is almost 3 times. The auxetic design is therefore more flexible than the one with positive angles, with a maximum value of the shear modulus occurring when the cell angle is of 30 ° and the curvature ratio assumes the value of 0.8.

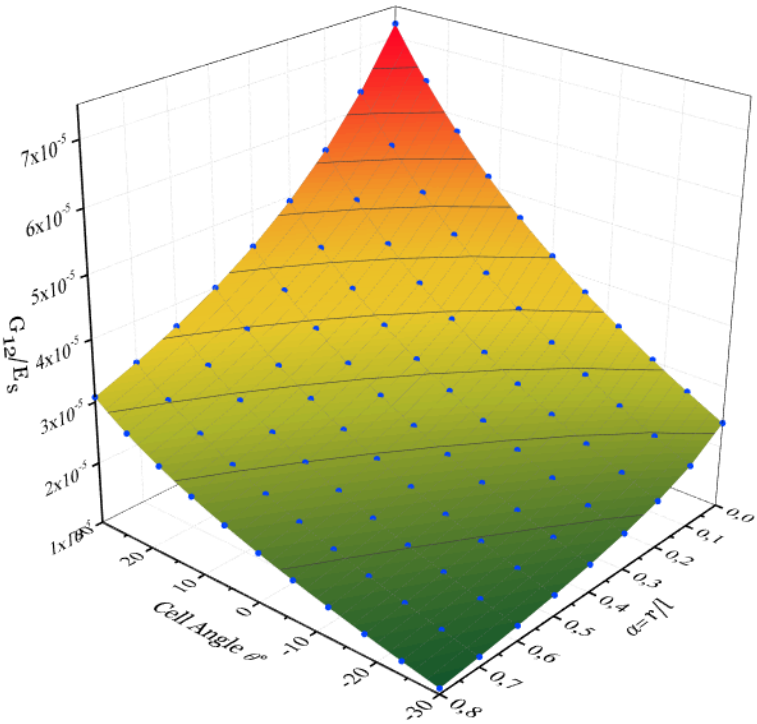

Figure 10: 3D representation of an analytical simulation of the shear modulus G_{12}/E_s versus cell angle θ for different normalized radius α for (β=a/*l*=1, γ=*t*/*l* =0.05).

3.4 Comparison between analytical model and Finite Element simulations

Table 1 summarizes the analytical and numerical results related to the uniaxial constants (Young's moduli and Poisson's ratio) for two curvature values (r/l = 2/30, r/l = 10/30) and for different cell configurations (auxetic and conventional). The results are all quite close, nevertheless the FE ones are slightly higher. Moreover, it is also worth of notice that the FE results obtained using the beam elements are closer to the analytical ones than those obtained by using shells (relative errors of 4.80% for shell elements and 4.46 % for beams ones - Table 1). In the case of the Poissons' ratios the maximum discrepancy is 5.24 % when using shell elements, and 3.74 % for the case of beams.

For the normalised shear modulus G_{12}/Es (Fig 11), a maximum error of about 4.0 % was found between the numerical simulation and the values of equation (Eq. 21) of the analytical calculation. The G_{12}/Es increase with the increase of θ from -30 to 30 degrees.

This confirms the ability of the analytical approach to estimate the mechanical properties of the cellular structure at a very low computational cost.

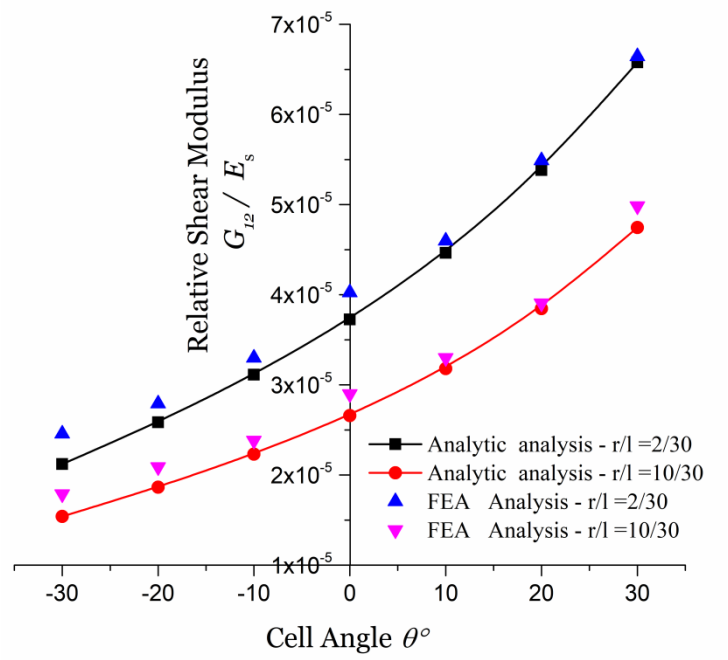

Figure 11: Normalized shear modulus G_{12}/Es versus cell angle for normalized radius of curvature (α =0.2) (Predicted by refined model and FEA).

3.5 The effect of the curvature of walls (r/l) on the anisotropy

The effect of the curvature on the anisotropy of the honeycomb is important, especially for zero-cell angles (i.e., vertical ribs). For θ equals to 0° and an increase of the curvature ratio α from 0 to 0.30, a very sharp 85% drop of the anisotropy (E_1/E_2) is observed, after which the variation is slower until α equal to 0.6. A less dramatic change in the anisotropy of the honeycomb is however obtained for honeycombs with a cell angle of θ = +30°, with a loss of 45% when the parameter α passes from 0 to 0.6. Unlike the previous two configurations, a 400% increase in anisotropy is noted for a negative angle θ of -30° (auxetic behaviour).

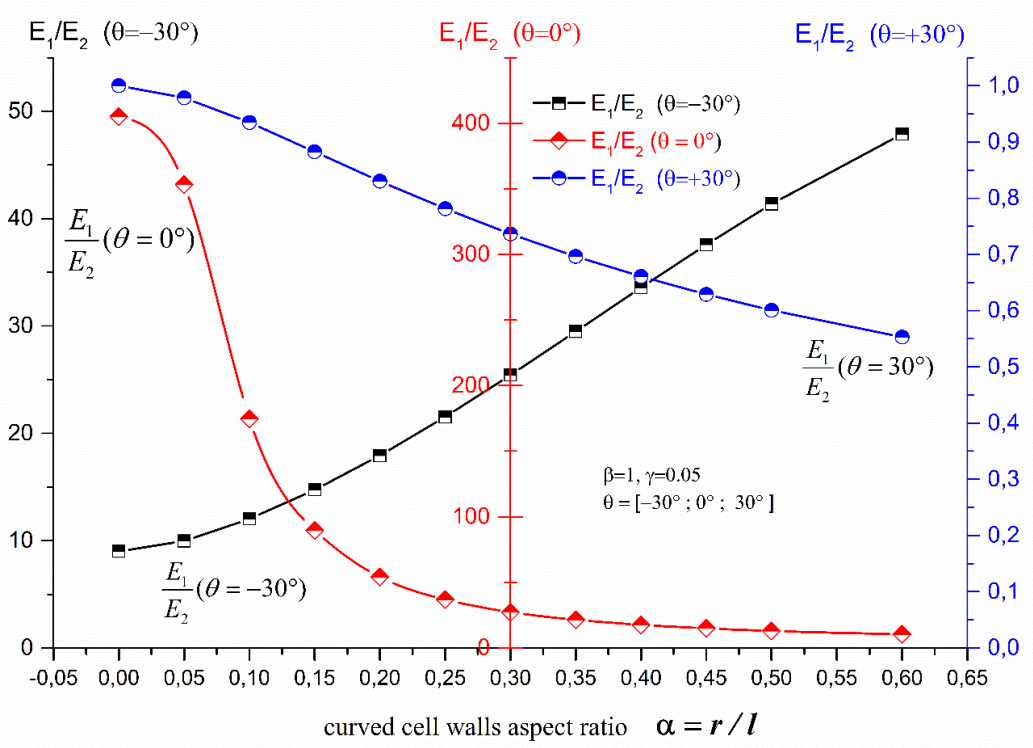

Figure 12 : The evolution of the anisotropy versus the curvature ratio of walls (r/l).

4. Conclusions

The aim of this work is to understand the effect of the internal angles and curvature of the cell wall on the mechanical behaviour of a new honeycomb cell design using an analytical framework and finite element modelling. In addition, the mechanical properties of the cellular structure were evaluated by introducing the effects of bending and transverse shear and axial forces.

The results found showed that curved walls had a significant effect on the elastic properties of cellular structures:

The moduli of elasticity E_1, E_2 and G_{12} decrease with increasing radius of curvature.

The behaviour of the cell becomes less anisotropic when the relative curvature of the walls increases except for the negative internal angles.

The consideration of different deformation mechanisms (bending-shear-stretching) tends to reduce the effective modulus of elasticity in the plane of the honeycombs.

The behaviour becomes less auxetic with the growth of the radius of curvature *r* for negative internal angles.

The shear modulus reduces with increasing radius of curvature and reaches its maximum value for the cell angle of +30°.

The modulus of elasticity E_1 is maximum for an internal angle and radius of zero curvature (vertical walls).

The Poisson's ratio ν_{12} values decrease with increasing radius of curvature for both configurations.

The elastic constants of the lattice with curved walls and calculated via the analytical model show a significant increase of the in-plane compliance compared to the classical regular hexagonal honeycomb [1] [30].

This study also highlights the difference in terms of results when using different classes of elements in finite element simulations for these honeycomb structures. The presence of curvature also makes it possible to design configurations with a positive Poisson's ratio even for the internal angles of the negative cells and makes this honeycomb design attractive for specific mechanical applications.

Acknowledgements

The Authors would like to acknowledge the Directorat General For Scientific Research and Technological Development (DGRSDT) – Algeria for supporting the project.

5. References

[1] Gibson LJ, Ashby MF. Cellular solids structure and properties. 2nd ed. UK: Cambridge University Press; 1997.

[2] ALMUT POHL « Strengthened corrugated paper honeycomb for application in structural elements » PhD thesis of Sciences- Dipl.-Ing. Technische Universitat Wiene

[3] E. Harkati, N. Daoudi, and all. In-plane elasticity of a multi re-entrant auxetic honeycomb Composite Structures 180 (2017) 130–139

[4] E. Harkati, Nour El-Houda Daoudi, Chames Eddine Abaidia, Abderrezak Bezazi, and Fabrizio Scarpa "The Elastic Uniaxial Properties of a Center Symmetric Honeycomb with Curved Cell

Walls: Effect of Density and Curvature " Physica status solidi-b Volume 254, Issue 12 December 2017.

[5] Bezazi A, Scarpa F, Remillat CA. Novel centre symmetric honeycomb composite structure. Compos Struct 2005;71(3–4):356–64.

[6] A. Bezazi, C. Remillat, P. Innocenti, F. Scarpa. In-plane mechanical and thermal conductivity properties of a rectangular–hexagonal *honeycomb* structure. Composite Structures, Volume 84, Issue 3, July 2008, Pages 248-255.

[7] Silva MJ, Hayes WC, Gibson LJ. The effects of non-periodic microstructure on the elastic properties of two-dimensional cellular solids. Int J Mech Sci 1995;11:61–77.

[8] Grima JN, Cauchi R, Gatt R, Attard D. Honeycomb composites with auxetic out-of-plane characteristics. Compos Struct 2013;106:150–9.

[9] Körner C, Liebold-Ribeiro Y. A systematic approach to identify cellular auxetic materials. Smart Mater Struct 2015;24:025013.

[10] Evans KE, Nkansa MA, Hutchinson IJ, Rogers SC. Molecular network design. Nature 1991;353:124 [9] Sun Y, Pugno NM. In plane stiffness of multifunctional hierarchical honeycombs with negative Poisson's ratio sub-structures. Compos Struct 2013;106:681–9.

[11] Whitty JPM, Alderson A, Myler P, Kandola B. Towards the design of sandwich panel composites with enhanced mechanical and thermal properties by variation of the in-plane Poisson's ratios. Compos Part A 2003;34:525–34.

[12] Pozniak AA, Kaminski H, Kedziora P, Maruszewski B, Strek T, Wojciechowski KW. Anomalous deformation of auxetic constrained square. Rev Adv Mater Sci 2010;23(2):169–74.

[13] Lim TC. Auxetic materials and structures. Singapore: Springer; 2015.

[14] Lakes RS. Foam structures with a negative Poisson's ratio. Science 1987;235:1038-40.

[15] Almgren RF. An isotropic three-dimensional structure with Poisson's ratio=-1. J Elast 1985;15:427–30.

[16] Lira C, Innocenti P, Scarpa F. Transverse elastic shear of auxetic multi re-entrant honeycombs. Compos Struct 2009;90:314–22.

[17] Scarpa F, Tomlin PJ. On the transverse shear modulus of negative Poisson's ratio honeycomb structures. Fatigue Fract Eng Mater Struct 2000;23:717–20.

[18] Nkansah ME, Evans KE, Hutchinson IJ. Modelling the mechanical properties of an auxetic-molecular network. Model Simul Mater Sci Eng 1994;2:337.

[19] Gibson LJ, Ashby MF, Zhang J, Triantafillou TC. Failure surfaces for cellular materials under multiaxial loads- I. Modelling. Int J Mech Sci 1989;31 (9):635–63

[20] Masters and Evans. Models for the elastic deformation of honeycombs. Compos Strut 1996;35:403–22.

[21] Sajad Arabnejad, Damiano Pasini : Mechanical properties of lattice materials via asymptotic homogenization and comparison with alternative homogenization methods. International Journal of Mechanical Sciences Volume 77, December 2013, Pages 249-262.

[22] C. Lira, F. Scarpa, Y.H. Tai, J.R. Yates « Transverse shear modulus of SILICOMB cellular structures » Composites Science and technology 71 (2011) 1236-1241.

[23] S. Balawi, J.L. Abot, "A refined model for the effective in-plane elastic moduli of hexagonal honeycombs", journal of Composite Structures 84 (2008) 147–158

[24] Sardar Malek, Lorna Gibson: Effective elastic properties of periodic hexagonal honeycombs. Mechanics of Materials, Volume 91, Part 1, December 2015, Pages 226-240.

[25] ABAQUS, version CEA 6.10-1 reference manuals- Dassault Systemes,Providence,R.I:Abaqus Inc.,2010.
[26] L. Al Bâchi, Modélisation numérique et expérimentale du comportement des matériaux sandwiches appliqués à l'aéronautique, Thèse de l'ENI de Tarbes, 2002.

[27] Chamis C C., R. A. Aiello, L.N. Murthy, "Fiber composite sandwich thermo structural behaviour: Computational simulation", Journal of composite technology & research 1988, vol. 10, pp. 93-99.

[28] Jorg Hohe, Wilfried Becker. Effective mechanical behavior of hyperelastic honeycombs and two-dimensional model foams at finite strain : International Journal of Mechanical Sciences, Volume 45, Issue 5, May 2003, Pages 891-913
[29] H. Jopek, T. Strek,. Effective mechanical properties of concentric cylindrical composites with auxetic phase Phys Status Solidi B 2015, 252, 1551.issue7.

[30] L J Gibson, M A Ashby, G S Schajer and C I Robertson, The mechanics of two-dimensional cellular materials, Proc. R. Soc. Lond. A382, Volume 25-42 (1982).